BEST AVAILABLE IMAGES

Defective images within this document are accurate representations of the original documents submitted by the applicant.

Defects in the images may include (but are not limited to):

- BLACK BORDERS
- TEXT CUT OFF AT TOP, BOTTOM OR SIDES
- FADED TEXT
- ILLEGIBLE TEXT
- SKEWED/SLANTED IMAGES
- COLORED PHOTOS
- BLACK OR VERY BLACK AND WHITE DARK PHOTOS
- GRAY SCALE DOCUMENTS

IMAGES ARE BEST AVAILABLE COPY.

As rescanning documents *will not* correct images, please do not report the images to the Image Problem Mailbox.

PCT WORLD INTELLECTUAL PROPERTY ORGANIZATION
International Bureau

INTERNATIONAL APPLICATION PUBLISHED UNDER THE PATENT COOPERATION TREATY (PCT)

(51) International Patent Classification 6 : G06T 11/00, A61B 6/03 — A1

(11) International Publication Number: WO 98/30980

(43) International Publication Date: 16 July 1998 (16.07.98)

(21) International Application Number: PCT/SE98/00029

(22) International Filing Date: 13 January 1998 (13.01.98)

(30) Priority Data:

9700072-3	14 January 1997 (14.01.97)	SE
9700437-8	10 February 1997 (10.02.97)	SE

(81) Designated States: JP, US, European patent (AT, BE, CH, DE, DK, ES, FI, FR, GB, GR, IE, IT, LU, MC, NL, PT, SE).

Published
With international search report.
Before the expiration of the time limit for amending the claims and to be republished in the event of the receipt of amendments.

(71) Applicants *(for all designated States except US)*: EDHOLM, Paul [SE/SE]; Arbetaregatan 50, S-582 52 Linköping (SE). ERIKSSON, Jan [SE/SE]; Fridtunagatan 5, S-582 12 Linköping (SE). MAGNUSSON-SEGER, Maria [SE/SE]; Leopolds gata 23, S-584 37 Linköping (SE). TURBELL, Henrik [SE/SE]; Furirgatan 25 A, S-581 12 Linköping (SE).

(71)(72) Applicant and Inventor: DANIELSSON, Per-Erik [SE/SE]; Hedborns gata 30, S-584 37 Linköping (SE).

(54) Title: TECHNIQUE AND ARRANGEMENT FOR TOMOGRAPHIC IMAGING

(57) Abstract

Complete helical cone-beam scanning and non-redundant data acquisition are obtained for three-dimensional tomographic imaging of infinitely long objects. The minimum sized two-dimensional detector window is bounded by two consecutive turns of the helix. The ray source exposes all object points during a rotation of exactly 180 degrees when seen from the points themselves. Only one-dimensional filtering is employed in the reconstruction. Rebinning to parallel beams, as seen along the axis of rotation, allows for especially simple procedures without any need for pre-weighting or magnification factors. As a special case, the invention is applicable to helical fan-beam scanning with one-dimensional detector arrays.

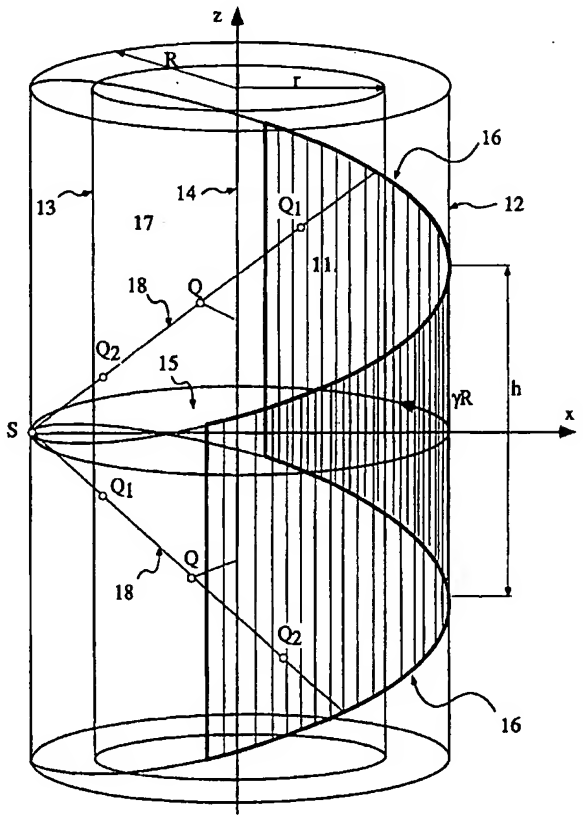

FOR THE PURPOSES OF INFORMATION ONLY

Codes used to identify States party to the PCT on the front pages of pamphlets publishing international applications under the PCT.

AL	Albania
AM	Armenia
AT	Austria
AU	Australia
AZ	Azerbaijan
BA	Bosnia and Herzegovina
BB	Barbados
BE	Belgium
BF	Burkina Faso
BG	Bulgaria
BJ	Benin
BR	Brazil
BY	Belarus
CA	Canada
CF	Central African Republic
CG	Congo
CH	Switzerland
CI	Côte d'Ivoire
CM	Cameroon
CN	China
CU	Cuba
CZ	Czech Republic
DE	Germany
DK	Denmark
EE	Estonia
ES	Spain
FI	Finland
FR	France
GA	Gabon
GB	United Kingdom
GE	Georgia
GH	Ghana
GN	Guinea
GR	Greece
HU	Hungary
IE	Ireland
IL	Israel
IS	Iceland
IT	Italy
JP	Japan
KE	Kenya
KG	Kyrgyzstan
KP	Democratic People's Republic of Korea
KR	Republic of Korea
KZ	Kazakstan
LC	Saint Lucia
LI	Liechtenstein
LK	Sri Lanka
LR	Liberia
LS	Lesotho
LT	Lithuania
LU	Luxembourg
LV	Latvia
MC	Monaco
MD	Republic of Moldova
MG	Madagascar
MK	The former Yugoslav Republic of Macedonia
ML	Mali
MN	Mongolia
MR	Mauritania
MW	Malawi
MX	Mexico
NE	Niger
NL	Netherlands
NO	Norway
NZ	New Zealand
PL	Poland
PT	Portugal
RO	Romania
RU	Russian Federation
SD	Sudan
SE	Sweden
SG	Singapore
SI	Slovenia
SK	Slovakia
SN	Senegal
SZ	Swaziland
TD	Chad
TG	Togo
TJ	Tajikistan
TM	Turkmenistan
TR	Turkey
TT	Trinidad and Tobago
UA	Ukraine
UG	Uganda
US	United States of America
UZ	Uzbekistan
VN	Viet Nam
YU	Yugoslavia
ZW	Zimbabwe

Technique and arrangement for tomographic imaging

Background

This invention was first described in **[Dan97a]**. A two-dimensional *detector* **11** and a point-shaped *ray source* (e g X-ray) S are assumed to move synchronously around the object in a helical trajectory as shown in Figure 1. In a medical tomograph the helical source movement is achieved by translating the patient through the rotating source-detector gantry with constant speed. Two-dimensional projections are acquired (detected) at arbitrarily short intervals along the trajectory. The detector consists of a large number of sensors (detector elements) which are evenly spaced and placed in a plane or, as in Figure 1, on the surface of the *helix cylinder* **12**. Although the *rotation axis* **14** is normally horizontal in medical tomographs, rather than vertical as in Figure 1, we will adopt the following convention. In the sequel, *vertical* means a direction parallel to the rotation axis **14** (the z-axis) in Figure 1, while *horizontal* means a direction parallel to the *xy-plane* **15**.

A projection consists primarily of intensity measures for the incoming rays to a detector element. The logarithms of these primary data represent the sum of the attenuation along the rays, i.e. line integrals over the three-dimensional attenuation function f we want to retrieve. But to be able to reconstruct f from its projections in a correct way, all points in the object have to be fully exposed and the projection data utilized in a balanced way. Thus, if back-projection is used for the reconstruction, projections from all projection angles must be available and brought in with the correct weight to obtain what is called exact reconstruction. Also, the projection data have to be filtered correctly to compensate for the inherent low-pass filtering in the projection-back-projection procedure.

In the literature several mathematically **exact** methods have been proposed for reconstruction from cone-beam projections. In most cases these methods demand that the object is of finite extension, i.e. restricted in size, so that its total projection never falls outside the available detector. Unfortunately, this requirement is not realistic in most cases of computer tomography, e.g. when one is to reconstruct a full body, or long objects in general. Traditionally, 1D-detector arrays are made large (wide) enough to cover the object across its maximum width. However, for several reasons, it is out of question to extend these 1D-detectors to 2D-detectors, which cover the patient from head-to-toe. Instead, in the foreseeable future, available 2D-detectors will be used to cover and record projections of a **section of a long object.**

Today, three-dimensional volume data are reconstructed slice-by-slice. The patient is translated slowly (typically 2 mm/sec) while the X-ray source and a one-dimensional detector array are synchronously and continuously rotated at speeds of around 1 r/sec. Relative to a patient which is not moving, the source and detector are then performing a helical movement with very low pitch, say, 2 mm. The reconstruction employs a modified versions of traditional 2D-reconstruction methods for circular scanning of a single slice. However, with the given numbers, it takes approximately 100 sec to fetch data for a 200 mm long section of the body. During this time, due to breathing and other body functions, the body is not fully at rest which blurs the reconstructed object. A second drawback is that the anode of the X-ray tube is subjected to severe strain and extreme temperatures during longer exposure times.

In a 1D-detector system the major part of the generated photons are collimated away without being utilized, while a 2D-detector system is able to utilize a substantial part of these otherwise wasted photons. Hence, by using a 2D-detector with, say, n parallel 1D-detectors in the above example, the velocity can be increased to $2n$ mm/sec and the scanning time reduced to $100/n$ sec. Alternatively, speed can be traded for strain on the X-ray source so that, for instance, if the photon flow is halved, the velocity is more moderately increased to n mm/sec and the scanning time reduced to $200/n$ sec. However, in any case it is no longer possible to perform the reconstruction using conventional 2D-methods since the projection rays are no longer, not even approximately, in the same plane during one turn of the source trajectory.

Prior Art

Circular source trajectory

A well-known method for inexact reconstruction from cone-beam projections taken along a circular path was proposed in **[Feld84]**. The 2D-detector is placed on a planar surface and extended horizontally to cover the width of the object. The width of the object and its distance to the source defines the maximum *fan-angle* γ_{max} of the source-detector system. In the vertical direction the planar detector is limited by two horizontal lines. Along the vertical axis where these lines are closest to the source we find the maximum *cone-angle*. The image reconstruction consists of the following steps taken for each detector recording. All corrections of geometrical and radiometric nature, including the ever necessary logarithm computation have been left out here for the sake of brevity.

1. *Pre-weighting of the recorded detector data with a factor that is proportional to the cosine of the angle between the central ray and the ray that originated the detected value.*
2. *Filtering with traditional ramp-filtering techniques along each horizontal detector row.*
3. *Back-projection along the original ray in which process the filtered detector value is multiplied with a so called magnification factor which depends on the distance between the ray source and the object point to receive a contribution from the ray.*

This method gives perfect results for image slices in, or close to the mid-section of the object. For slices which have been subjected to more oblique rays at higher cone angles, the image quality deteriorates.

Helical source trajectory. Non-exact methods

Extensions of [Feld84] to helical source paths were first proposed by **[Wang93]**. Here, the planar 2D-detector is given a vertical extension large enough to ascertain that every point is exposed to the source at least once for every projection angle during a full 360 degree source rotation. The effect of this requirement is that for any given projection angle an object point will be exposed by the source from **various numbers of source positions**; at least one but often many more, depending on the given fan-angle, cone-angle and detector size. This has to be taken into account during the back-projection. Hence, [Feld84] is employed in [Wang93] but augmented with the following rule.

3a. During the back-projection, for a certain projection angle, among all possible source positions which illuminate an object point, contributions are accepted only from the position which is closest to the actual point in the z-direction.

A way to achieve a more efficient and balanced exposure of the object points was proposed in **[Scha96]**. Here, the detector is located (wrapped) onto the surface of the *source cylinder* **41**, which in Figure 4 is seen to be centered in **S**. The radius of this cylinder equals the source-detector distance, which is different from the radius R of the helix cylinder **12**. The helix cylinder is coaxial with the *object cylinder* **13** in Figure 1 which is defined by the maximum object width r. In [Scha96] the detector is limited in the vertical direction by two horizontal circles (cross-sections) of the source cylinder **41**. However, it is not quite clear what the minimum or optimal height is to be recommended for the detector. In the horizontal direction the detector is limited by two vertical lines, set to let the detector cover the object cylinder. In the following we may use Figure 1 to clarify some prior art such as this, even if the detector arrangement in our invention is different from the detector in [Scha96] and [Scha97].

The main novelty in [Scha96] is the introduction of *complementary projections*. These are projection data captured at the source cylinder **41**, but sorted and resampled (rebinned) with respect to where the rays from the source are reaching the helix cylinder **12**. Assume for the moment that the source is moving along the helix **16** while the object and the helix cylinder is fixed. All rays from various source positions on the same turn, reaching a fixed point on the helix cylinder, is said to be a complementary fan-beam and the projection data for this fan-beam is created during the rebinning. The set of such not quite horizontal and not quite planar fan-beams, with rays fanning out from points on a vertical line on the helix cylinder, constitute a complementary projection. These are employed in the following reconstruction procedure.

1. Pre-weighting of the recorded detector data with a factor that is proportional to the cosine of the angle between the central ray in the projection and the ray that originated the detected value .

2. Re-binning to complementary projections.

3. Filtering of the original as well as the complementary projections with traditional ramp filtering techniques along each horizontal detector row. Because of the non-planar detector this filter is slightly different from the filter employed in [Feld84].

4. For each projection angle, filtered projection data are back-projected along the rays. The values are multiplied with magnification factors which depend on the distance between the

point and ray source. All such values, from original as well as complementary cone-beam source positions, are averaged into one single contribution that is accumulated to the object point.

We notice that the detector arrangement in [Scha96] does not secure a perfectly balanced exposure of the object points. During the back-projection event, for each rotation angle, there is a similar situation as in [Wang93] where the object points are exposed from one or several source positions. The difference is that in [Scha96] all these projection data from both original and complementary projections are utilized and averaged together during the backprojection.

[Scha97] proposes another reconstruction technique that is claimed to be more computationally efficient. The detector system is identical to the one in [Scha96] with two horizontal truncating circles on the surface of the source cylinder **41**. The reconstruction consists the following steps.

*1. Rebinning to **oblique parallel projections**.*
2. Pre-weighting of the recorded detector data with a factor that is proportional to the cosine of the angle between the ray that originated the detected value and the central ray.
*3. Reconstruction of one horizontal slice from **generalized projections**. The latter can be seen as the result of imaginary projection rays running within the horizontal slice.*
3.1. Computation of Fourier domain contributions to this slice for one generalized projection at every projection angle.
3.1.1. Computation of Fourier domain contributions for each "detector" position in one generalized projection.
3.1.1.1. Multiplication of projection data (from all source positions that send oblique rays through the slice in this position) with a pre-computed set of weights, which are Fourier series components derived from an adopted interpolation function.
3.1.1.2. Summation of the contributions for each Fourier component to obtain a single set, a truncated Fourier transform for each ray in this detector position of this generalized parallel projection.
3.1.2. Computation of the Fourier transform (FFT) along the projection for all these truncated Fourier components to obtain a kind of truncated 2D Fourier transform contribution for each generalized parallel projection.
3.1.3. Multiplication of the Fourier transform of this generalized projection with a ramp filter.
3.2. Merging of filtered data from all projection angles in the 2D Fourier space of the

horizontal slice and resampling with a space-invariant interpolation filter.

3.3. Application of an inverse 2D Fourier transform (FFT).

3.4. Compensating for imperfect interpolation in the Fourier domain by post-weighting the result with the inverse interpolation function, in accordance with the well known gridding technique.

The first rebinning step is best understood if the source, the detector, and the object **17** is pictured as seen from above. From there, the cone-beams will be seen as fan-beams. The rebinning in step 1 above is equivalent to sorting projection data into sets where data from this point of view are produced not by fan-beams but from parallel beams. The term *oblique parallel projections* stems from the fact that the rays are parallel when seen from above, but in general non-parallel and oblique to the horizontal plane. To understand the following steps it is now recommendable to imagine a planar, virtual detector **122** as in Figure 12 placed vertically on the rotation axis in the middle of the object. There are several source positions which produce the rays for this projection. Since the real detector on **41** is truncated horizontally and the source positions are located along the helix **16**, the effective area of this virtual detector does not have a left-right symmetric shape. The upper and lower boundaries **131** and **132** are curved and tilted as shown in Figure 13. This is an important difference to the perfectly rectangular shape of the corresponding virtual detector **72** in Figure 10 for the present invention. The net effect is that in [Scha97] a varying number of source positions generate fan-beams which penetrate a given slice under various oblique angles. All of these contribute to the result in the above ingenious but rather complicated computation steps 3.1.1.1 and 3.1.1.2. In the present invention we will find one and only one such fan-beam.

Helical source trajectory. Exact methods

An exact method for reconstruction of a limited sector, a **Region Of Interest (ROI)** of a long object was proposed in **[Tam95]** and **[Eber95]**. The helical scanning covers the full vertical extension of the ROI but has to be complemented with two circular scans at top and bottom, respectively. The detector is placed on a planar surface, just as in [Feld83] and [Wang93] but the detector *window* is limited to the area between two consecutive turns of the source trajectory **16** as in Figure 1. The upper and lower truncating lines on the detector *plane* are therefore neither horizontal, straight, nor left-right symmetric. The arguments for the specific extension of the detector stem from a well-known completeness condition for Radon planes which carries over to the following reconstruction technique. In essential aspects this method is an outgrowth from **[Gra87]**.

1. *From each 2D-projection, partial contributions to the derivative of Radon transform values are computed by means of line integration along a multitude of lines in the planar detector. This requires that we select a specific object point to be the origin of a 3D coordinate system.*
2. *When the scanning is complete, that is when the helical trajectory has covered the intended target region of the object (ROI), all these partial contributions are sorted and coplanar partial contributions are summed.*
3. *The result is resampled into a regular grid in the Radon transform space of the ROI of the object function.*
4. *Filtering with a derivative filter.*
5. *3D back-projection which takes place as two consecutive 2D back-projection steps.*

Generally speaking, this reconstruction is more complicated and costly that the previous ones. Also, the rhythm of the reconstruction procedure is affected by the chosen size of the ROI. It does not feature an even flow of identical procedures repeatedly taking place for every new projection regardless of the length of the object. The two extra circular scans are highly unwanted since they break the smooth and continuous translation-rotation motion of the helical part. However, the method is optimal in one respect. For a given pitch of the helix it utilizes a minimum sized detector.

The Invention

The present invention utilizes the same optimal, minimum cost two-dimensional detector geometry as proposed in [Tam95], characterized by an exposure window which is limited vertically by the two nearest turns of the helical source trajectory. However, both the motivation for and the exploitation of this detector window differs greatly from the ones given in [Tam95] and [Eber95]. To explain the specific virtue of this exposure window, we refer again to Figure 1, which shows a perspective view of a source **S**, a detector **11** wrapped around the helix cylinder **12**, and inside this an object cylinder **13**. In the sequel, unless stated otherwise, we assume that the object cylinder is rotating counter-clock-wise as shown around the z-axis and translated upwards in a right-handed helix, while the source **S** and the detector **11** are fixed in the space (x, y, z).

Figure 2 shows the arrangement as seen from above, while Figure 3 shows the detector window unwrapped and rolled out on a plane. Note that Figures 1 and 3 are consistent only if the rays in Figure 3 are understood to be coming from the source towards the viewer. Figure 4 shows the detector placed on the *source cylinder* **41** centered in **S** and having a radius which is twice as large as the helix cylinder **12**. The figures 1, 2, 3, and 4 presented here are in principle, although not in detail, identical to figures 1, 2, 3, and 4 in [Dan97a].

As mentioned, the 2D-detector **11** in Figure 1 is wrapped onto the helix cylinder **12**. Unwrapped and rolled out on the plane of the sheet, the same detector surface **11** in Figure 3 is seen to be bounded by four straight lines, two vertical ones **31** and **32**, and two slanted ones **33** and **34**. Within this area the object **17** is projected, i.e., rays from the cone-beam source reaches active detector elements. Horizontally, this area has to be extended to cover the object cylinder **13**, which translates to a certain width, or fan angle γ_{max}, as seen from the source. As an example we have assumed that this object cylinder has a radius $r = \frac{R}{\sqrt{2}}$ where R is the radius of the helix cylinder **12**. This means that horizontally on **12**, the detector covers a rotation angle of 180 degrees out of 360, and that seen from the source the detector **11** covers a fan angle from - 45 to +45 degrees. In principle the detector may be extended to a full turn which then has a fan-angle from -90 to +90 degrees and would allow for an object cylinder that extends all the way to the helix. The slanted lines **33** and **34** are intersecting the cylinder surface **12** at the slope

$$\tan \varepsilon = \frac{v}{\omega R} = \frac{h}{2\pi R} \qquad (1)$$

where v is the vertical translation velocity, ω is the angular velocity for the rotation, and h is the pitch of the helix.

At the core of the invention is the following property of the detector-exposure window. **Every point in a cylindrical long object, with a radius that fits inside the boundaries of the detector window, will be exposed (projected) during a rotation angle which is exactly 180 degrees, seen from the actual point in the object.** A more formal proof of this property was given in **[Dan97b]** but is left out here for the sake of brevity. A conjecture of this new sufficiency condition is that **as soon as one point or a set of points (i.e. a part of the long object) has been fully exposed in the above sense, the reconstruction of this part can take place.** This is in contradiction to the situation in [Tam95] and [Eber95]] where the whole ROI has to be exposed to make the Radon space complete before the actual reconstruction is commenced.

An example of this 180 degree exposure is the line **18** in Figure 1. It contains the three object-points $Q_1 - Q - Q_2$ and it is shown in two positions where the exposure starts and ends, respectively. Note that the end points of this line is sliding and touching the outer cylinder so that during the rotation, both ends will coincide with the source S. Any such line will be called a **π-line**. This line is also shown in Figure 2 in the same two positions.

Assume as before that the object is moving upwards and rotating counter-clockwise when seen from above. In the detector window of Figure 3 the line $Q_1 - Q - Q_2$ crosses the lower boundary **34** as a single point at Q_{in}. After a rotation with the angle $\pi + 2\gamma$ around the axis **14**, this line will be seen as a single point again from the source leaving the detector at Q_{out} on the upper boundary **33**. Clearly, between entrance and exit the source has rotated exactly 180 degrees as seen from any point on this line. Since we have chosen this line quite arbitrarily, the same thing is true for all points in the object which belong to fully exposed π-lines. In Figure 2 and Figure 3, but not in Figure 1, we have inserted another π-line $P_1 - P - P_2$. In the fixed source-detector system of Figure 2 this line P enters and exits in positions which are exactly the reverse of the corresponding positions for the line Q. The line P is therefore closer to the source than line Q during its exposure, which takes place during a rotation angle of $\pi - 2\gamma$. The points on line P travels over the detector surface along different and shorter curves as shown in Figure 3, but seen from any of these points, the source rotates around them exactly 180 degrees.

It was shown in [Dan97b] that every object point belongs to one and only one π-line. Therefore, the detector system in Figure 1 gives us a complete and perfectly balanced data capture for every point and hence also for the whole object. Furthermore, from the conjecture above follows that it should be possible to reconstruct the object at the same pace as an incremental part (each new set of π-lines) of the long object is fully exposed.

The physical implementation and placement of the detector can of course be made in various ways as indicated in Figure 4. For instance, it may be placed on the helix cylinder **12** itself, on the source cylinder **41** or on a plane **42**. In any case, the detected and utilized data must be restricted to the window defined by Figure 3.

In our invention, using the same detector data, the elaborate reconstruction in [Tam95] and [Eber95] will be replaced by a much simpler procedure. To describe this procedure, we do not have to limit the ongoing scanning and reconstruction to a predetermined ROI, nor do we have to specify a 3D origin for the process. Instead, scanning and reconstruction is like a constantly ongoing flow, in principle without beginning or end, where each new projection is absorbed and incorporated seamless to the previous result. For this purpose, the following general reconstruction procedure for every new projection is found in [Dan97a].

1. *Rebinning*
2. *Pre-weighting (depending on rebinning and detector type)*
3. *One-dimensional filtering with a ramp-filter across the detector (where the filter design is dependent on rebinning and detector type)*
4. *Back-projection along incoming ray direction with magnification factors, depending on type of rebinning as well as on detector type: plane, cylindrical, etc.*

A special case of this procedure is rebinning to parallel projections which we will describe in more detail. Figure 5 shows a straight side-view of Figure 1 with six rays **51**, **52**, **53**, **54**, **55**, and **56** coming from the source S positioned at the x-axis. Figure 6 shows a view from above where the object is fixed and the source and detector is rotating. With the source in the position S_α we observe three fan-beams **61**, **62**, and **63** (seen as rays in this view), which comprises the six rays in Figure 5 and which produce the three projection sets $t(\alpha, \gamma_1)$, $t(\alpha, 0)$, $t(\alpha, -\gamma_1)$. The two outer rays are parallel to two other rays, **64** and **65**, coming from two other source positions which produce the projections $t(\alpha + \gamma_1, 0)$ and $t(\alpha - \gamma_1, 0)$, respectively. Clearly, we may resample our projection data so that data from

such parallel fan-beams (seen as rays) are brought together. This can be done with either of the following two equivalent assignments.

$$\left[p(\alpha+\gamma,\gamma) \Leftarrow t(\alpha,\gamma)\right] \equiv \left[p(\beta,\gamma) \Leftarrow t(\beta-\gamma,\gamma)\right] \qquad (2)$$

As shown in Figure 7 we are then free to see the data set $p(\beta, \gamma)$ as generated by a parallel beam in the β-direction. Without loss of generality, this direction is horizontal in Figure 7. Perpendicular to these rays we place a *virtual detector* **72** on a vertical plane.

The detector window **71** for the parallel projection in Figure 7 is unwrapped and rolled out into the sheet of Figure 8. Note that the complete detector positions for the parallel projection are put together from vertical lines **83**, **84**, and **85** each one stemming from different cone-beam detector positions. The resulting parallel beam detector area has the same slant as the cone-beam detector but is shortened with a factor of two in the γ-direction. The uppermost and lowermost part of the detector **81** and **82** in Figure 8 outlines another detector window included here for comparison only. To the best of our understanding, this window corresponds to the minimum size detector in [Scha96] and [Scha97] when mapped onto the helix cylinder **12**. For the given pitch = h and the given maximum fan angle γ_{max} the height of this detector window is

$$\frac{2v\left(\pi+\gamma_{max}\right)}{\omega R\cos\gamma_{max}} = \frac{h}{\cos\gamma_{max}}\frac{\pi+\gamma_{max}}{\pi} = h\left(\frac{1+\frac{\gamma_{max}}{\pi}}{\cos\gamma_{max}}\right) \qquad (3)$$

This formula indicates that the detector redundancy in [Scha96] and [Scha97] grows rather quickly for increasing fan-angles.

The rays in the parallel projection emanate from a set of **sources with vertical fan-beams,** located on a specific section of the helix. Rolled out in the plane of the sheet this part **73** of the source helix is superimposed on the detector **71** in Figure 8. It takes the form of a line with the same slant as the detector but with opposite sign. Because of this fact, in the present invention, the virtual detector **72** in the vertical mid-plane is bounded by a perfect rectangle with a width that equals the object cylinder diameter and a height which is exactly half the pitch = $h/2$. This is illustrated in Figure 9, where an upward tilt of the source path **73** is exactly compensated for by a downward tilt of the detector. Furthermore, since the distance from the virtual detector **72** to the source is everywhere identical to the distance to the real

detector, the real detector height h is always demagnified to exactly $h/2$ at the virtual detector. Figure 10 illustrates the second part of the rebinning-resampling procedure, namely from equidistant grid points in γ R to equidistant grid points in $y' = R\sin\gamma$.

The aforementioned property of the virtual detector area being a perfect rectangle is further illustrated in Figure 11, which shows three orthogonal views A, B, and C of the parallel projection system. Seven source positions are indicated. In A, B we can see the projection as a line **d-e** from the source positions S. Clearly, in view B we see that all the three points **S**, **d**, and **e** are on the helix. Furthermore, the plane of the virtual detector intersects the helix in two points which are exactly halfway between S and **d** at the upper ray **111** and halfway between S and **e** at the lower ray **112**. Therefore the height of the vertical detector is $h/2$ with its midpoint on the x-axis for any **S**. This proofs that the virtual detector is a rectangle with horizontal boundaries.

Thus, using the insight that there is a special detector window which delivers sufficient and non-redundant data, we capture cone-beam projection data on this detector and rebin them into parallel projection data to create an advantageous situation for the actual reconstruction. The complete procedure consists of the following three steps.

1. Rebinning to parallel projections as described by the Figures 6, 7, 8, 9, 10, and 11.
2. Filtering with a conventional ramp-filter along horizontal rows in the virtual detector plane.
3. Back-projection in the direction of the original rays using a constant magnification factor.

In the present invention, after parallel rebinning, the one-dimensional filtering takes place along horizontal rows in the virtual detector **72** of Figure 10. In [Scha96] and [Scha97] the filtering takes place along horizontal rows of a detector placed on the source cylinder arc **41** in Figure 4. Figure 13 shows this detector mapped onto the virtual detector plane **121**. The horizontal rows in the real detector are mapped onto curves in **121** which are neither horizontal nor straight. Clearly, filtering along such curves in the virtual detector plane rather than along horizontal rows will produce a rather different reconstruction result..

Even so, Step 3 in the above procedure may very well be replaced by a simplified version of the corresponding step 3 in [Scha97]: *Reconstruction of one horizontal slice from generalized projections.* The simplification is due to the perfectly balanced data capture in the present invention. We know a priori that there is one and only one source position that contributes to each detector position in the generalized projections as shown in Figure 9. Hence, there is no need to keep track of multiple exposure contributions, since there are neither missing nor

redundant data in any projection. The situation is different in [Scha97] which is illustrated in Figure 12 showing a vertical section of the parallel scanning system. The real detector **125** is much higher than in Figure 9 so that the virtual detectors **121**, **122**, and **123** for neighboring half turns overlap vertically. Therefore, in a vertical plane (such as the plane of the sheet) a horizontal slice of the object is partially illuminated not from one but from three source positions on the trajectory. This irregularly distributed redundancy in exposure is also reflected in Figure 13 which shows the virtual detector window in [Scha97] for the minimum sized detector. The upper and lower boundaries **131** and **132**, respectively, are the same as **81**, **82** in Figure 8, although mapped onto the virtual planar detector.

In the most likely physical embodiment of the 2D-detector arrangement proposed in this invention, the detector elements are placed onto the source cylinder **41**. See Figure 4. For moderate cone angles the detector elements are then facing the incoming rays rather straight on. For detectors made to cover high cone angles it might be more appropriate to mount the detector elements on the inside of a sphere centered in S. This would guarantee or at least make it more easy to secure that all detectors are facing the incoming rays correctly.

Figure 14 shows again the detector window **11** on the helix cylinder rolled out on the plane of the sheet. However, this time it is overlaid with the same the detector window mapped onto the source cylinder arc **41**.In its rolled out version, this detector appears in Figure 14 outlined as **141**. Considering the geometry of Figure 4, it might be more optimal to place the detector on the source cylinder arc **43** having the smallest possible radius close up to the object cylinder **13**. However, since the geometry of such a detector would conform exactly with **141**, we may discuss the geometry of **141** without loss of generality.

The detector **141** coincides with **11** in the middle but varies with γ so that the top-most and bottom-most point of the detector are found at

$$z_{top} = \frac{v}{\omega R}\frac{\pi + 2\gamma}{\cos\gamma} \quad \text{and} \quad z_{bottom} = \frac{v}{\omega R}\frac{\pi - 2\gamma}{\cos\gamma}, \tag{4}$$

respectively. The height H is then varying as

$$H(\gamma) = z_{top} + z_{bottom} = \frac{v}{\omega R}\frac{2\pi}{\cos\gamma} = \frac{h}{\cos\gamma} \tag{5}$$

where h is the pitch as before. Thus, data which are captured on the source cylinder have to be resampled from the unevenly sloping detector area in Figure 14 to the grid of the detector in Figure 3 (also shown in Figure 14), defined by vertical lines and evenly sloping lines with rhombus shaped detector elements. When projection data are resampled once more to the planar virtual detector in Figure 10, the final grid pattern will be perfectly rectangular.

An important special case for the present invention is when the detector **141** (and the pitch) of Figure 14 is reduced in height to a single row **150** of detector elements **151**, which is shown in Figure 15. We note that also in this special case will the height of the detector element increase with increasing fan angle as predicted by the above formula (5). Normally, the detector array in Figure 15 would no longer be considered as a two-dimensional detector but a one-dimensional array detector. One-dimensional array detectors are used in existing helical fan-beam tomographs for which the state-of-the-art is represented by **[King93]**. The detector is normally placed on the surface of a source cylinder **41**, although not designed as the one in Figure 15. Instead, the detector elements are of constant height and they are not placed in a slanted fashion but horizontally straight on the source cylinder surface.

As a consequence, to secure sufficient data, either the height of the detector elements have to be increased, as in formula (3) which decreases the resolution in the z-direction, or the pitch of the helix has to be decreased with the same factor, which reduces the scanning efficiency and increases the dose compared to the present invention. The scanning will also acquire much redundant data so that the accompanying reconstruction procedure has to employ elaborate weighting factors to compensate for multiple exposure. In essence, [King93] is a predecessor and the fan-beam counterpart to [Scha96]. Therefore, in helical fan-beam scanning, the present invention should have the same advantages compared to [King93] as we have found it to have when compared to [Scha96] and [Scha97]. Using the present invention with a detector designed and arranged accordingly, for instance as in Figure 15, the data capture will be complete and free of redundancy and the reconstruction procedure can be simplified to contain the three steps rebinning, one-dimensional ramp filtering, and backprojection with constant magnification factor.

References

[Dan97a] P.E.Danielsson, *"Förfarande och anordning för tomografering"*, Swedish Patent application No 9700072-3, filed Jan 14, 1997.

[Dan97b] P.E.Danielsson, Paul Edholm, Jan Eriksson, Maria Magnusson Seger, *"Towards Exact 3D-Reconstruction for Helical Scanning of Long Objects"*, Conf. Record from 1997 Int. Meeting on Fully Three-Dimensional Image Reconstruction, Nemacollin, PA, June 25-28, 1997.

[Feld84] L.A.Feldkamp, L.C.Davis, J.W.Kress, *"Practical Cone Beam Algorithms"*, Journal of Optical Soc.Am. vol. A6, pp. 612-619, 1984.

[Wang93] G.Wang, T.H.Lin, P.C.Cheng, D.M.Shinozaki,*"A General Cone-Beam Reconstruction Algorithm"*, IEEE Trans. on Medical Imaging, Vol. 12, pp. 486-496, 1993.

[Scha96] S.Schaller, T.Flohr, P.Steffen, *"A New Approximate Algorithm for Image Reconstruction in Cone-Beam Spiral CT at Small Cone Angles"*, Conference Record, IEEE Medical Imaging Conference, pp. 1703-1709, Nov. 1996, Anaheim, CA.

[Scha97] S.Schaller, T. Flohr, P. Steffen, *"New Efficient Fourier-Reconstruction Method for Approximate Image Reconstruction in Spiral Cone-Beam CT at Small Cone Angles"*, to be published in Proc. of SPIE Med. Imaging Conference, Newport Beach, CA, Feb.22-28, 1997.

[Tam95] K.C.Tam, *"Three-Dimensional Computerized Tomography Scanning Method and System for Large Objects with Smaller Area Detectors"*, US Patent 5,390,112, Feb. 14, 1995.

[Eber95] J.W.Eberhard; K.C.Tam, *"Helical and Circle Scan Region of Interest Computerized Tomography"*, US Patent 5,463,666, Oct. 31, 1995.

[Gra87] P.Grangeat, *"Mathematical Framework of Cone-Beam 3D Reconstruction via the First Derivative of the Radon Transform"*, in *"Mathematical Methods in Tomography"*, G.T.Herman, A.K.Luis, F.Natterer (editors), Lecture Notes in Mathematics, Springer, 1991.

[King93] K.F.King, A.H.Lonn, C.R.Crawford, *"Computed Tomographic Image Reconstruction Method for Helical Scanning Using Interpolation of Partial Scans for Image Construction"*, US Patent 5,270,923, Dec. 14, 1993.

CLAIMS

1. Arrangement and method for three-dimensional tomographic imaging of long objects, where the object to be investigated is subjected to simultaneous translation and rotation relative to the cone-beam ray source and the detector, characterized by a two-dimensional detector limited to a window opposite to the source, where this window is constrained to correspond to a surface area shaped as a parallelogram which is attached to a cylinder centered at the axis of rotation and passing through the source, and where the height of the window measured along the length of the cylinder equals the pitch of the helix and the width of the window is made to cover the maximum width of the object to be reconstructed, and where the upper and lower boundary of the window coincides with two consecutive turns of the source path relative to a fixed object, and where the reconstruction procedure is characterized by steps which include pre-weighting with a factor that depends on the angle of the ray that gave rise to the specific detector value, followed by filtering with a filter of type ramp-filter horizontally or near horizontally across the detector, followed by back-projection with a magnification factor along the direction of the rays that gave rise to the original detector values, and where the actual pre-weighting, the actual filter design, and the actual magnification factor depend on the physical embodiment given to the detector and which rebinning that has been employed to the detected data.

2. Arrangement and method for three-dimensional tomographic imaging of long objects, where the object to be investigated is subjected to simultaneous translation and rotation relative to the cone-beam ray source and the detector, characterized by a two-dimensional detector limited to a window opposite to the source, where this window is constrained to correspond to a surface area shaped as a parallelogram which is attached to a cylinder centered at the axis of rotation and passing through the source, and where the height of the window measured along the length of the cylinder equals the pitch of the helix and the width of the window is made to cover the maximum width of the object to be reconstructed, and where the upper and lower boundary of the window coincides with two consecutive turns of the source path relative to a fixed object, and where the reconstruction procedure is characterized by steps which for each incoming cone-beam projection includes rebinning to parallel projections as seen along the rotation axis and locating and resampling the rebinned data to a virtual detector plane on the rotation axis, followed by ramp-filtering along all horizontal rows in this detector plane, followed by back-projection in the direction of the original rays using a constant magnification factor.

3. Arrangement and method for three-dimensional tomographic imaging of long objects, where the object to be investigated is subjected to simultaneous translation and rotation

relative to the cone-beam ray source and the detector, characterized by a two-dimensional detector limited to a window opposite to the source, where this window is constrained to correspond to a surface area shaped as a parallelogram which is attached to a cylinder centered at the axis of rotation and passing through the source, and where the height of the window measured along the length of the cylinder equals the pitch of the helix and the width of the window is made to cover the maximum width of the object to be reconstructed, and where the upper and lower boundary of the window coincides with two consecutive turns of the source path relative to a fixed object, and where the reconstruction procedure is characterized by steps which for each incoming cone-beam projection includes rebinning to parallel projections as seen along the rotation axis and locating and resampling the rebinned data to a virtual detector plane in the rotation axis, followed by reconstruction of one horizontal slice at a time using generalized projections and Fourier transform technique.

4. Arrangement and method for three-dimensional tomographic imaging of long objects as in Claim 1, 2, or 3, characterized by an effective detector area that has an extension which correspond to the area exposed through the aforementioned window but is physically shaped in a different way and placed in a different position.

5. Arrangement and method for three-dimensional tomographic imaging of long objects as in Claim 4, characterized by a detector which is placed on a vertical plane.

6. Arrangement and method for three-dimensional tomographic imaging of long objects as in Claim 4, characterized by a detector which is placed on the surface of a cylinder with a vertical axis on the source S.

7. Arrangement and method for three-dimensional tomographic imaging of long objects as in Claim 4, characterized by a detector which is placed on the surface of a sphere centered on the source S.

8. Arrangement and method for three-dimensional tomographic imaging of long objects as in Claim 4, characterized by a detector which is placed on the surface of a cylinder, the axis of which is the axis of rotation.

9. Arrangement and method for three-dimensional tomographic imaging of long objects as in Claim 4, 5, 6, 7, or 8, characterized by a detector consisting of one single row of detector elements.

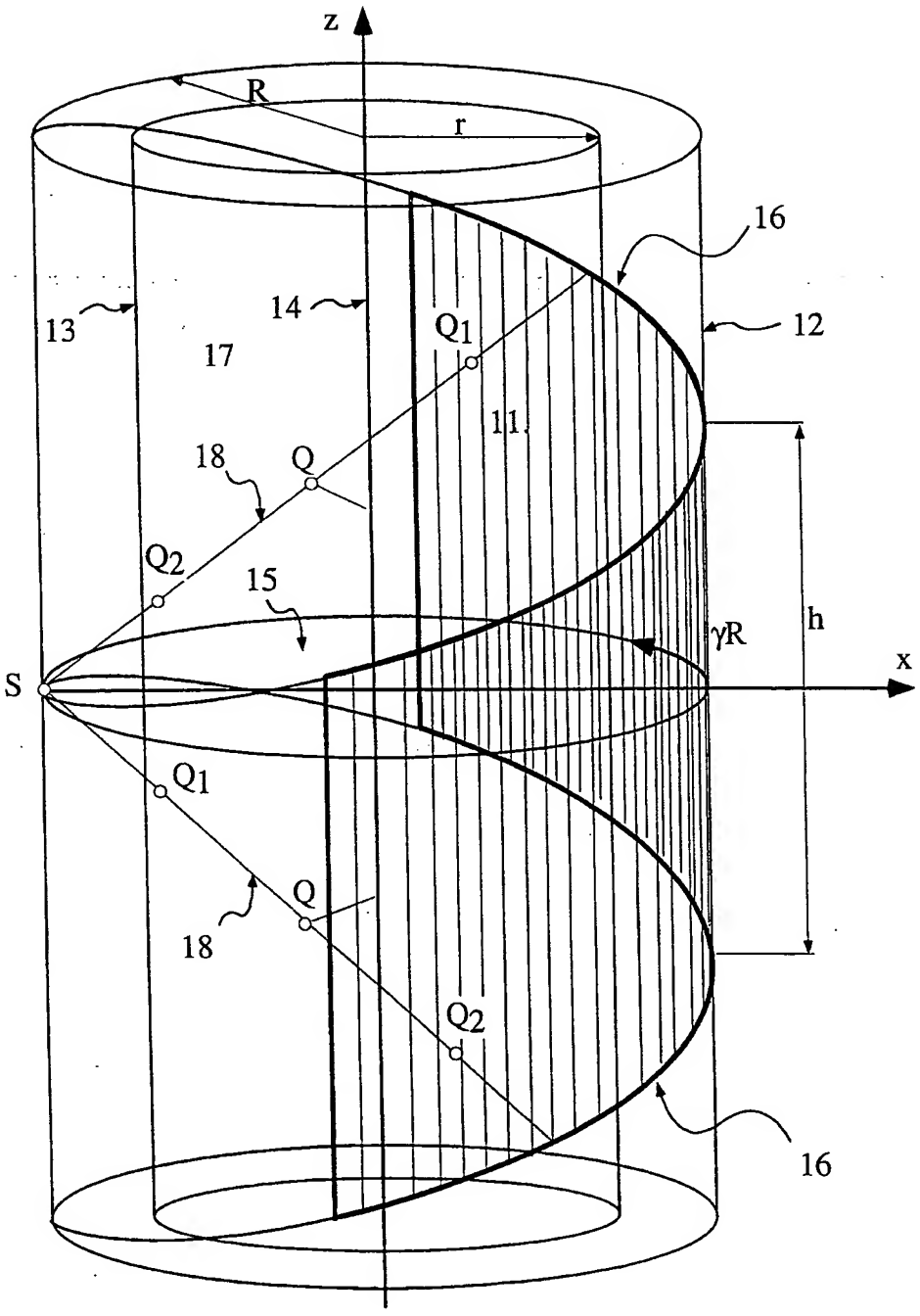

Figure 1

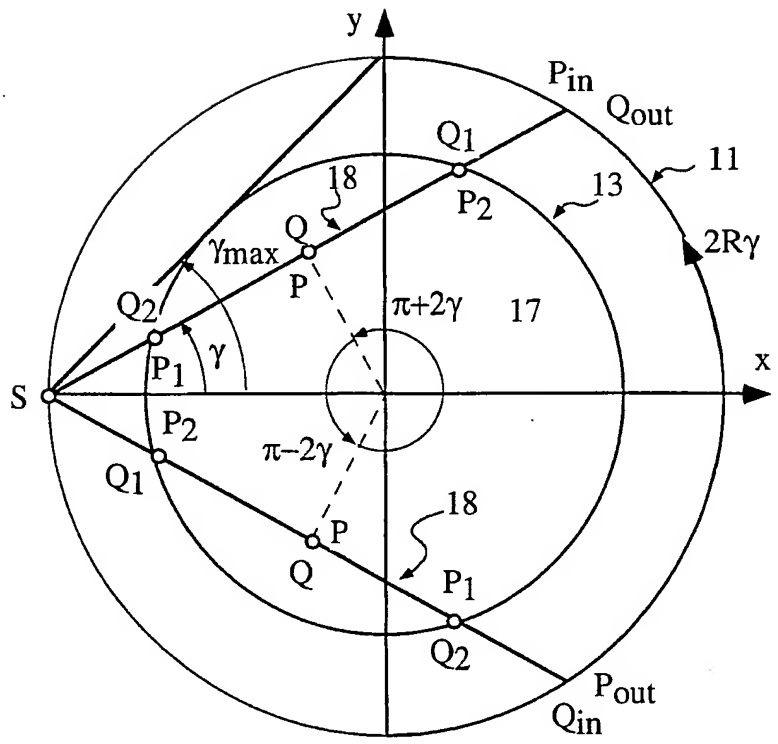
y
Pin
Qout
Q1
11
18
13
P2
Q
2Rγ
γmax
P
Q2
π+2γ
17
x
S
P1
γ
P2
π−2γ
Q1
18
P
Q
P1
Q2
Pout
Qin

Figure 2

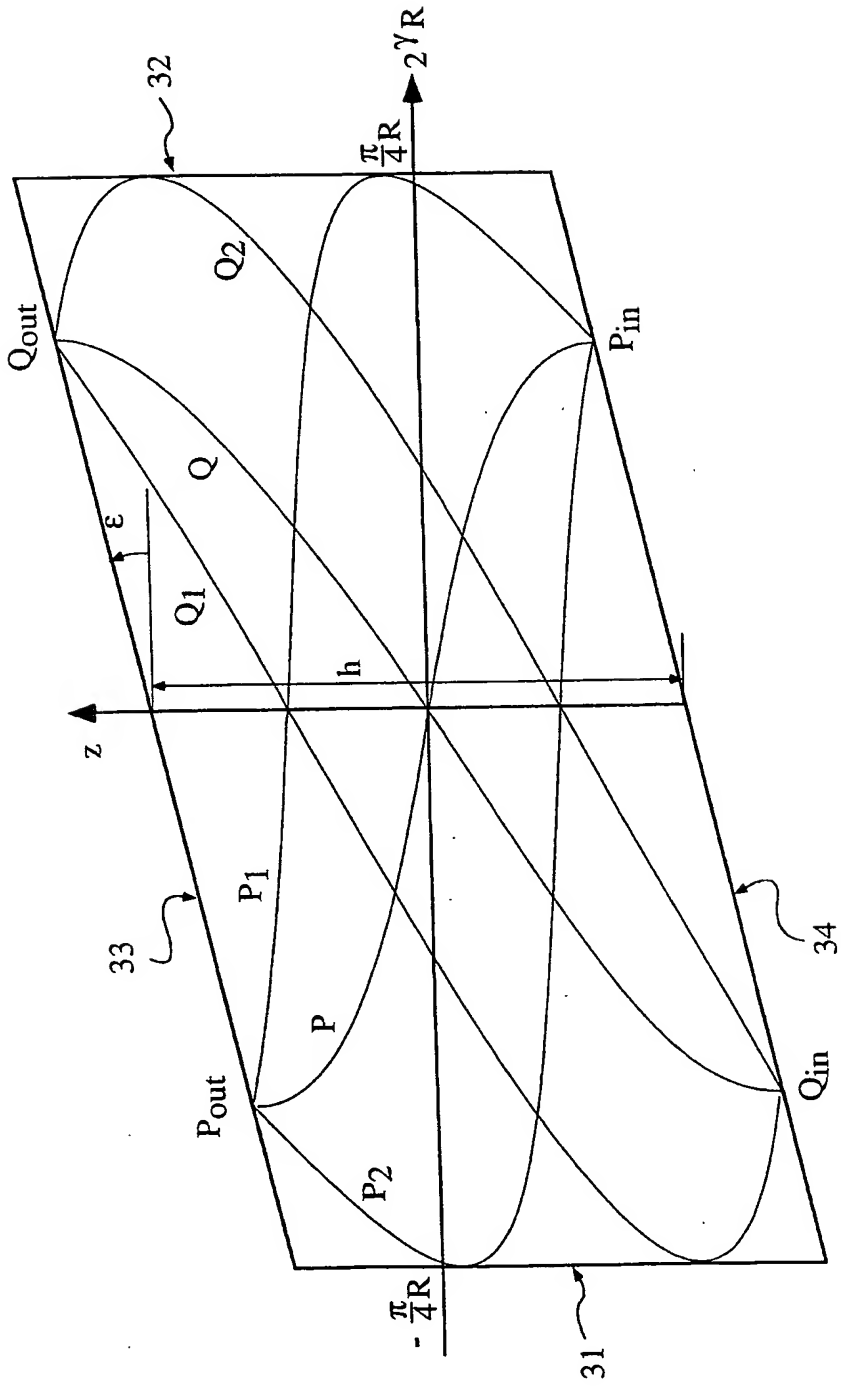
32
$2\gamma_R$
$\frac{\pi}{4}R$
Q_{out}
Q_2
P_{in}
Q
ε
Q_1
h
z
P_1
33
34
P
P_{out}
Q_{in}
P_2
$-\frac{\pi}{4}R$
31

Figure 3.

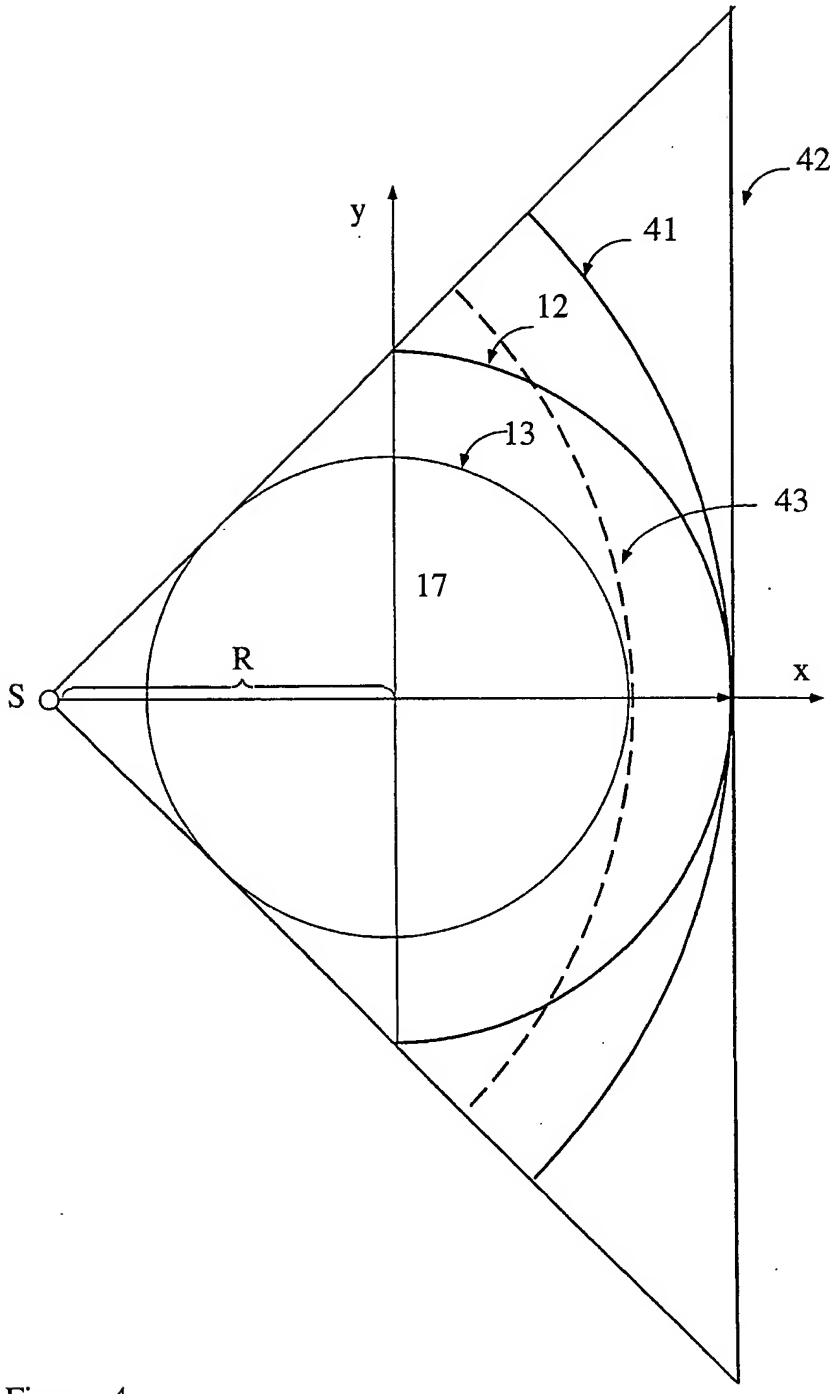

Figure 4

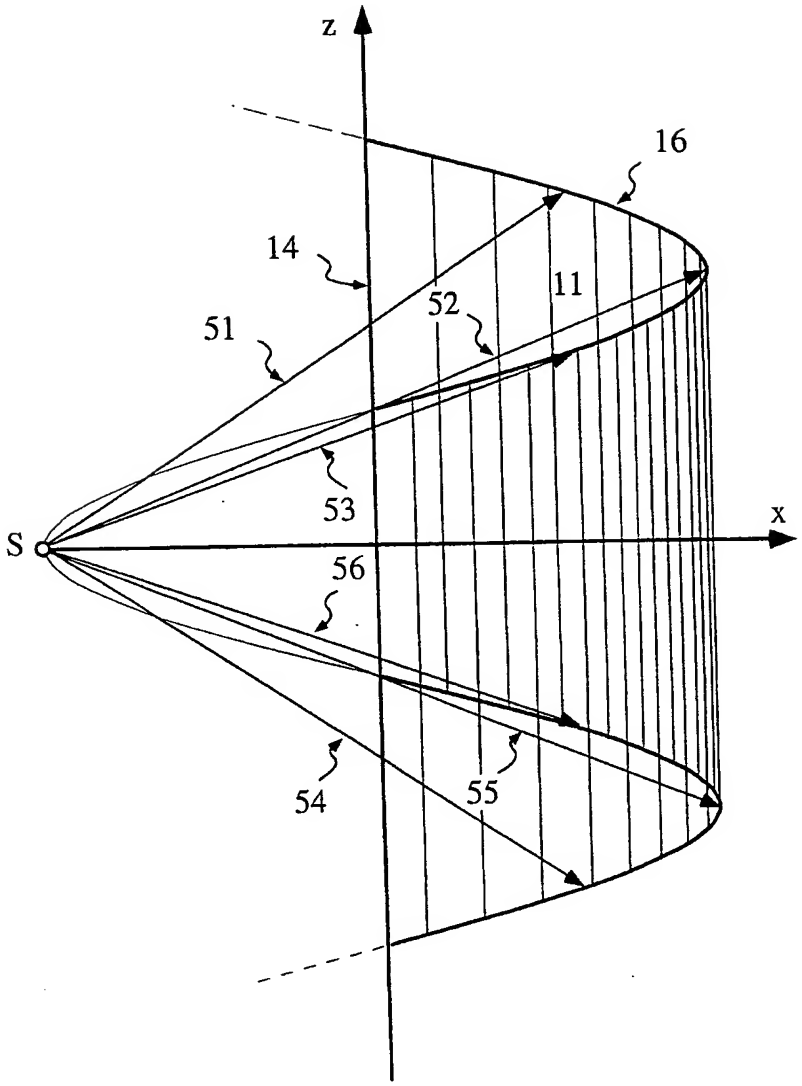

Figure 5

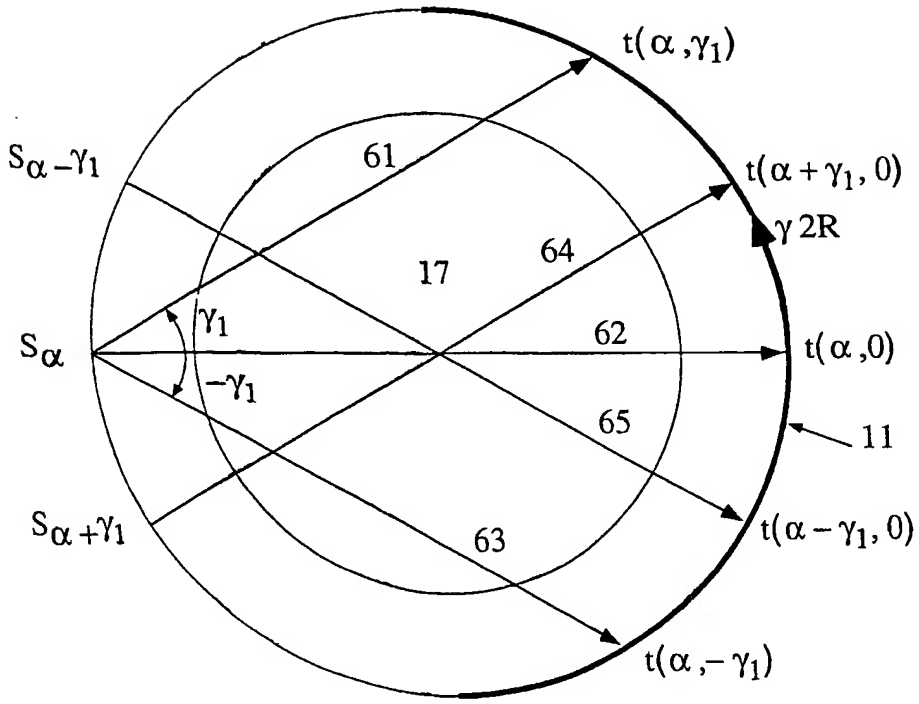
t(α ,γ1)
Sα –γ1
61
t(α + γ1, 0)
γ 2R
64
17
γ1
Sα
62
t(α ,0)
–γ1
65
11
Sα +γ1
63
t(α – γ1, 0)
t(α ,– γ1)

Figure 6

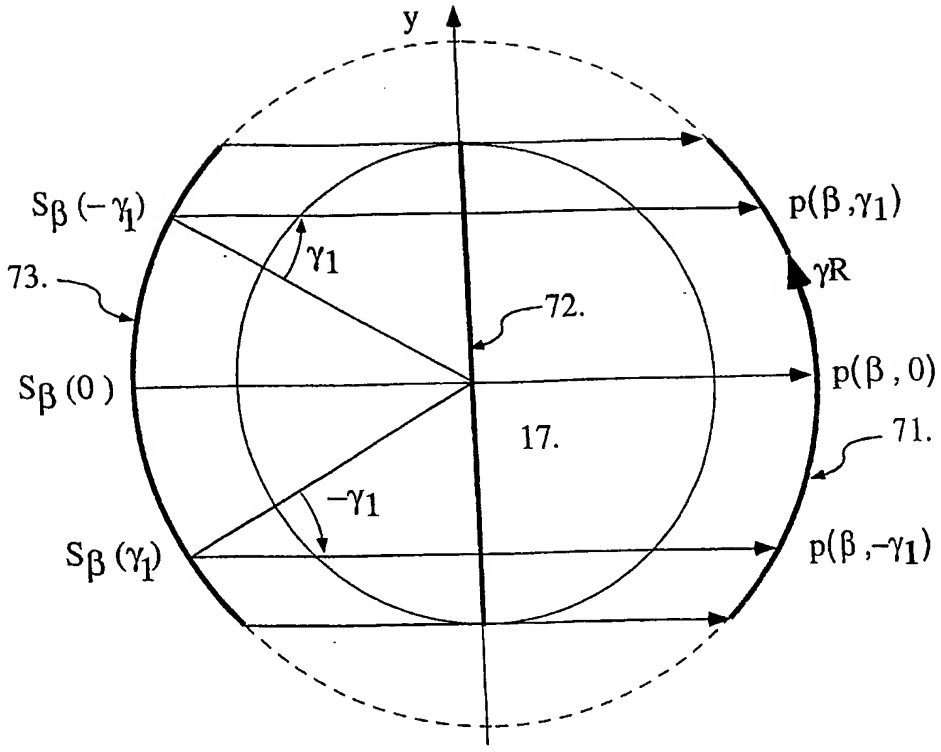

Figure 7

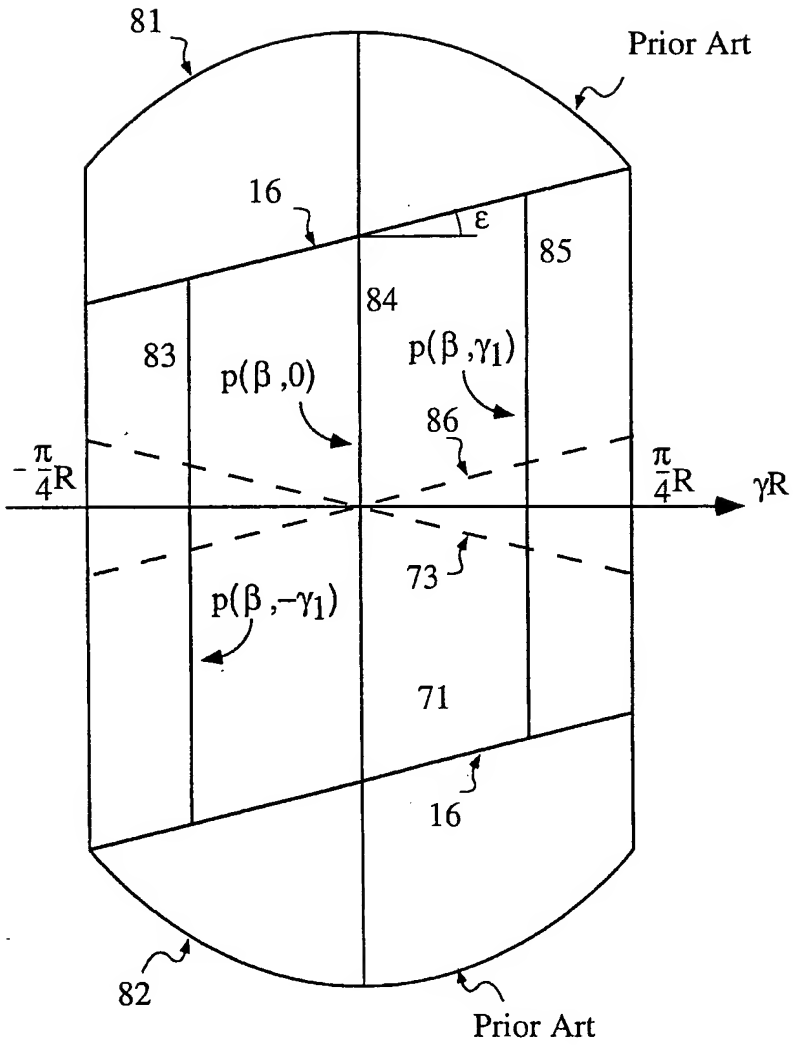
81
Prior Art
16
ε
85
84
83
p(β ,0)
p(β ,γ1)
86
-π/4R
π/4R
γR
73
p(β ,-γ1)
71
16
82
Prior Art

Figure 8

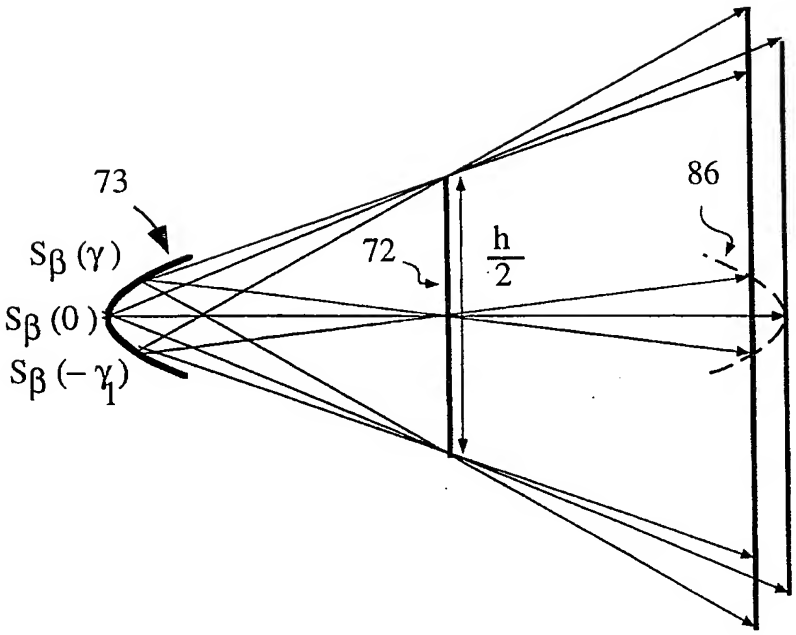

Figure 9

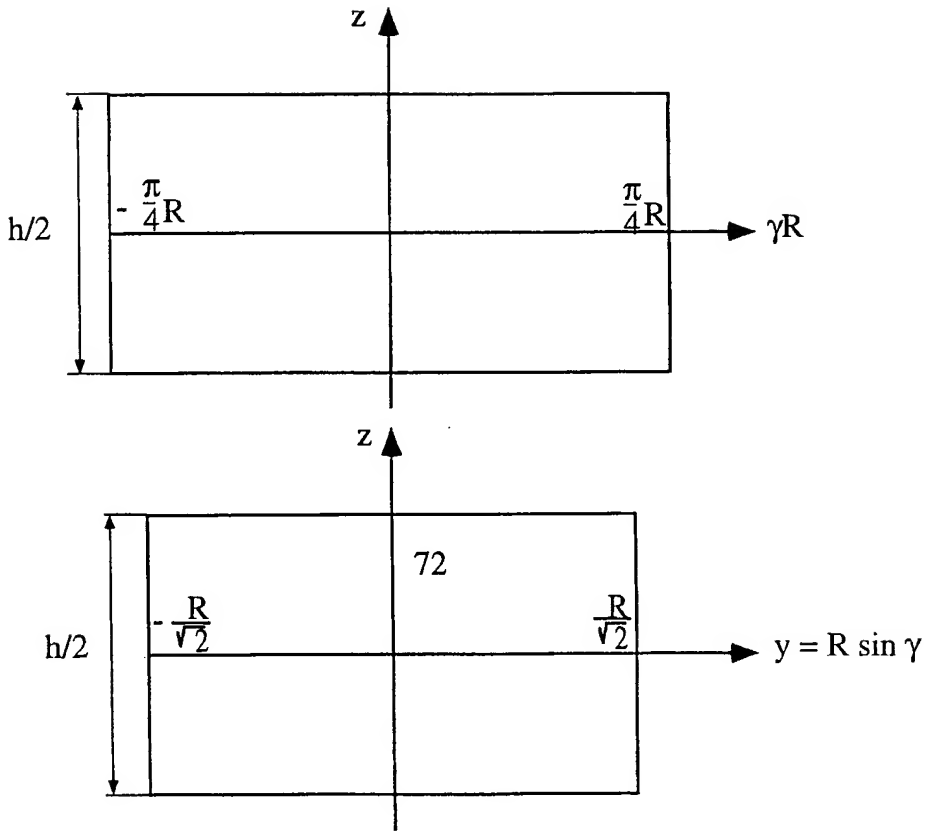
z
h/2
$-\frac{\pi}{4}R$
$\frac{\pi}{4}R$
γR
z
72
h/2
$-\frac{R}{\sqrt{2}}$
$\frac{R}{\sqrt{2}}$
y = R sin γ

Figure 10

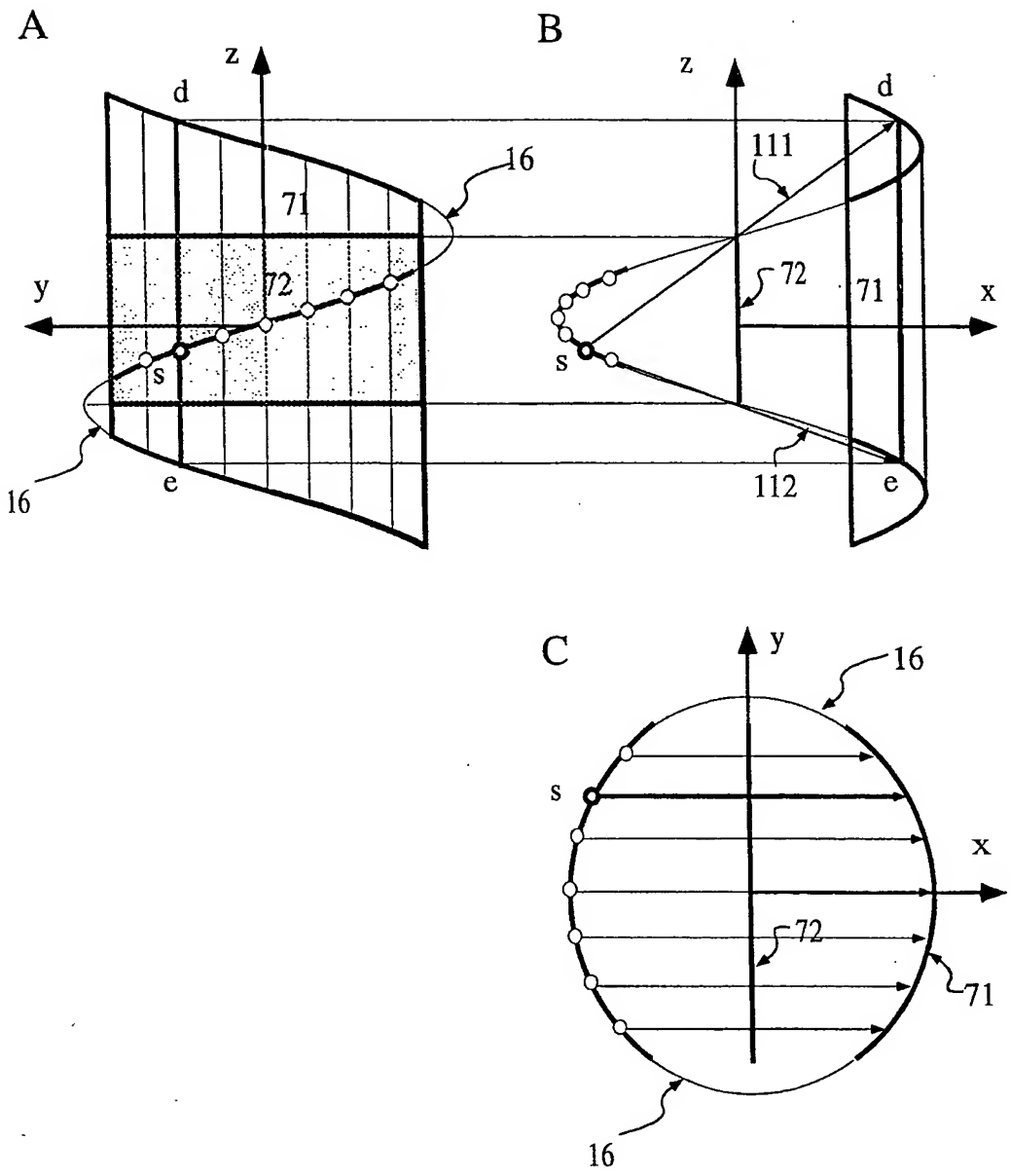

Figure 11

Prior Art

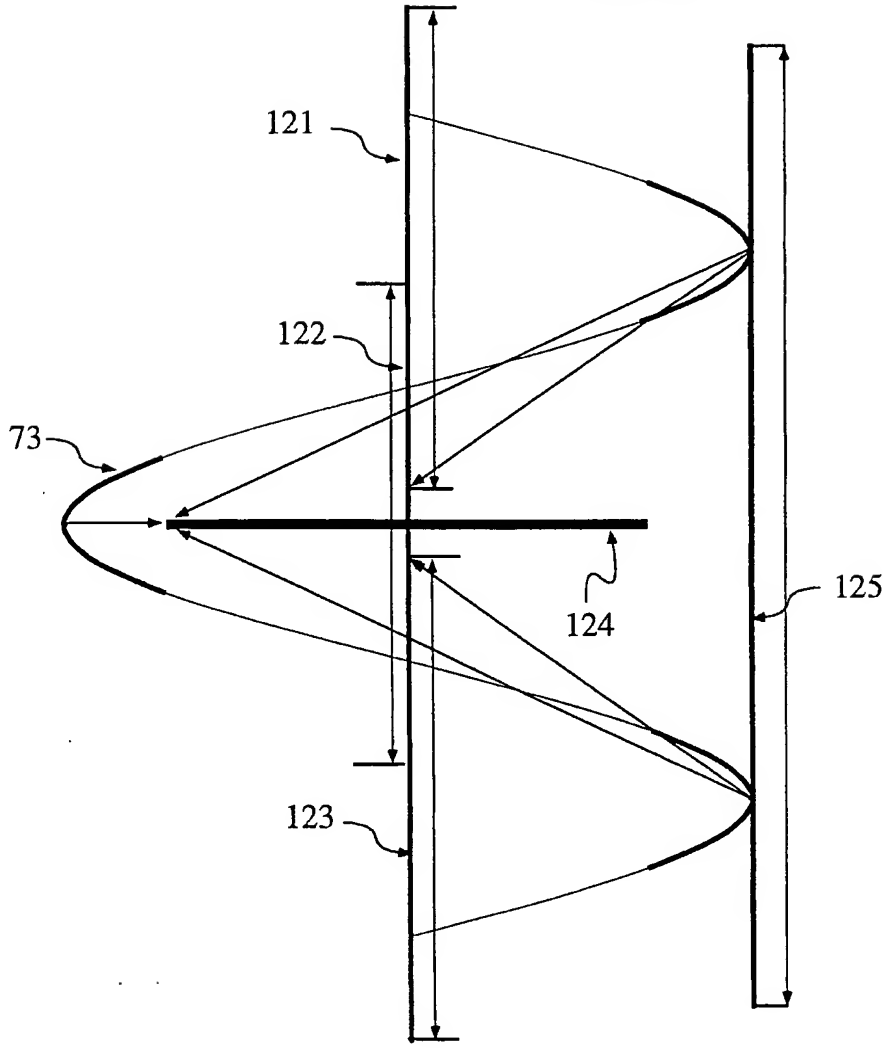

Figure 12

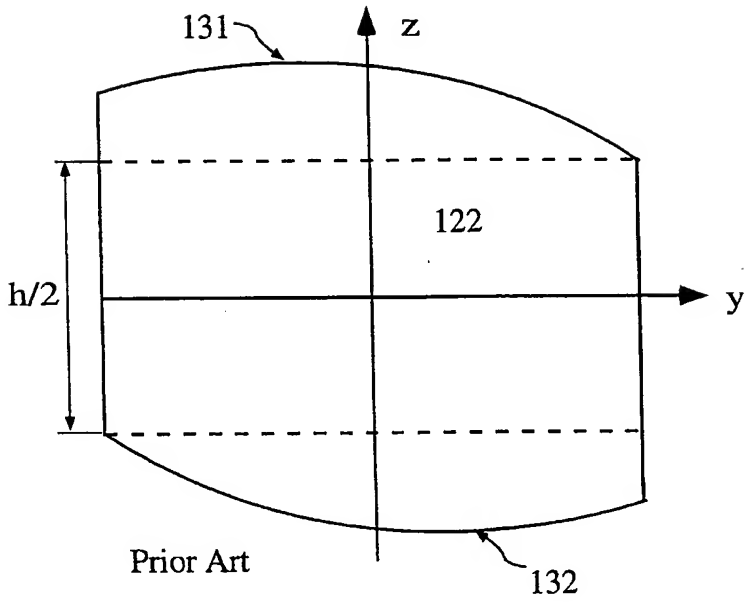

Figure 13

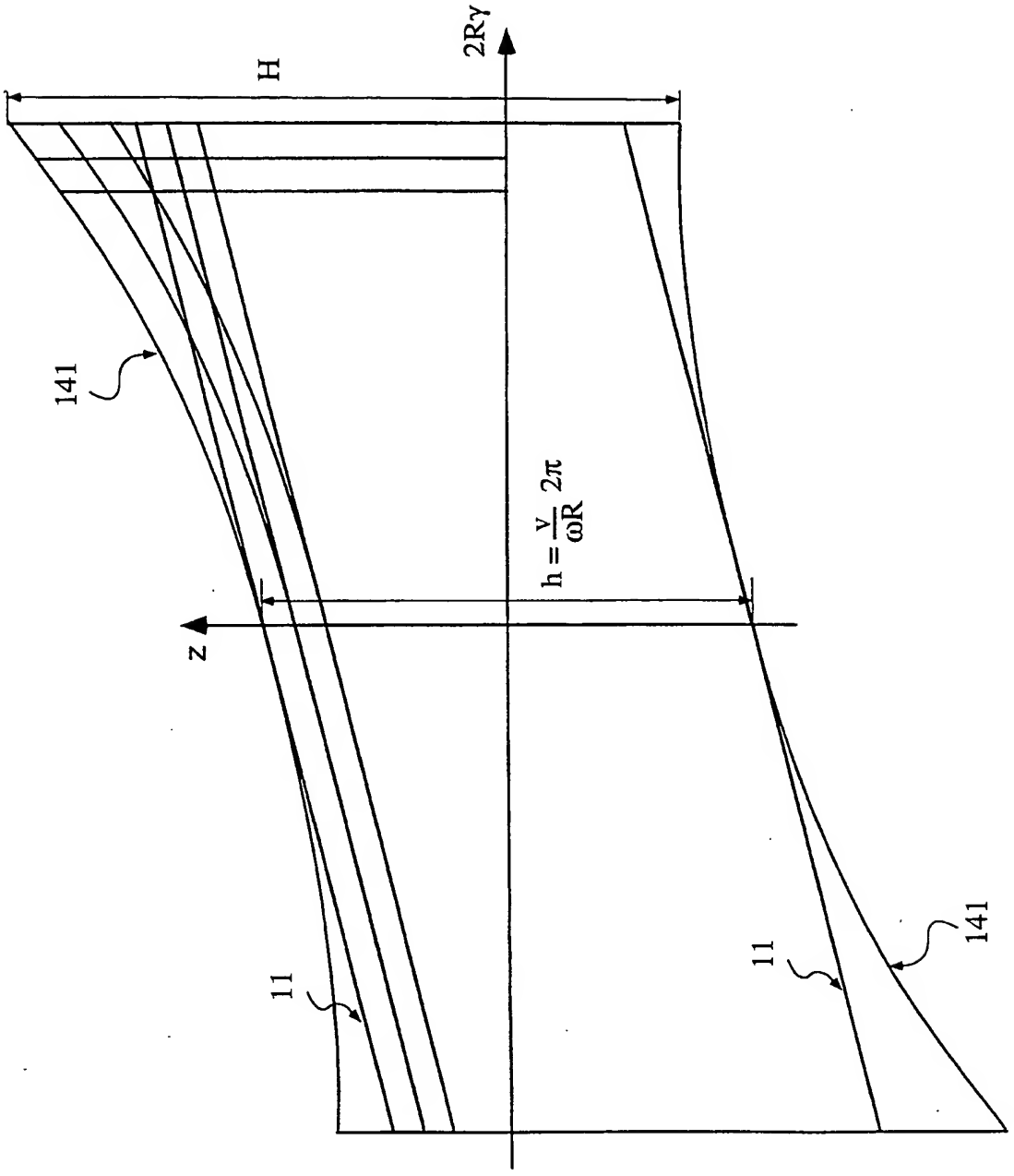

Figure 14

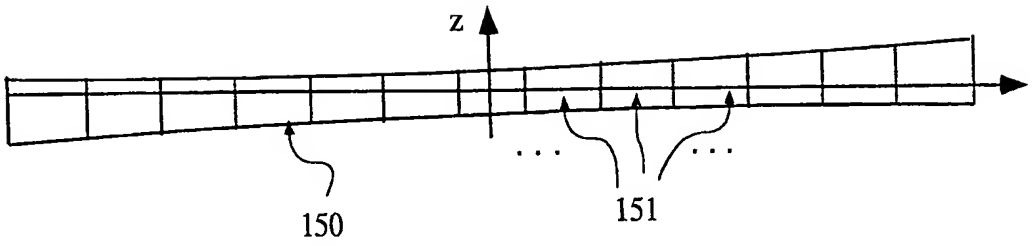

Figure 15

INTERNATIONAL SEARCH REPORT

International application No.
PCT/SE 98/00029

A. CLASSIFICATION OF SUBJECT MATTER

IPC6: G06T 11/00, A61B 6/03
According to International Patent Classification (IPC) or to both national classification and IPC

B. FIELDS SEARCHED

Minimum documentation searched (classification system followed by classification symbols)

IPC6: A61B, G06T

Documentation searched other than minimum documentation to the extent that such documents are included in the fields searched

SE,DK,FI,NO classes as above

Electronic data base consulted during the international search (name of data base and, where practicable, search terms used)

INSPEC, WPIL

C. DOCUMENTS CONSIDERED TO BE RELEVANT

Category*	Citation of document, with indication, where appropriate, of the relevant passages	Relevant to claim No.
A	US 5544212 A (DOMINIC J. HEUSCHER), 6 August 1996 (06.08.96), column 4, line 1 - line 36	1-9
A	US 5390112 A (KWOK C. TAM), 14 February 1995 (14.02.95), column 2, line 51 - column 3, line 57	1-9
A	IEEE Nuclear Science Symposium, Volume, 1996, (Anaheim CA), Stefan Schaller et al, "A New Approximate Algorithm for Image Reconstruction in Cone-Beam Spiral CT at Small Cone Angles" page 1703 - page 1709	1-9

[X] Further documents are listed in the continuation of Box C. [X] See patent family annex.

* Special categories of cited documents:
"A" document defining the general state of the art which is not considered to be of particular relevance
"E" erlier document but published on or after the international filing date
"L" document which may throw doubts on priority claim(s) or which is cited to establish the publication date of another citation or other special reason (as specified)
"O" document referring to an oral disclosure, use, exhibition or other means
"P" document published prior to the international filing date but later than the priority date claimed
"T" later document published after the international filing date or priority date and not in conflict with the application but cited to understand the principle or theory underlying the invention
"X" document of particular relevance: the claimed invention cannot be considered novel or cannot be considered to involve an inventive step when the document is taken alone
"Y" document of particular relevance: the claimed invention cannot be considered to involve an inventive step when the document is combined with one or more other such documents, such combination being obvious to a person skilled in the art
"&" document member of the same patent family

Date of the actual completion of the international search	Date of mailing of the international search report
28 May 1998	01 -06- 1998
Name and mailing address of the ISA/ Swedish Patent Office Box 5055, S-102 42 STOCKHOLM Facsimile No. +46 8 666 02 86	Authorized officer Malin Keijser Telephone No. +46 8 782 25 00

Form PCT/ISA/210 (second sheet) (July 1992)

INTERNATIONAL SEARCH REPORT

International application No.
PCT/SE 98/00029

C (Continuation). DOCUMENTS CONSIDERED TO BE RELEVANT

Category*	Citation of document, with indication, where appropriate, of the relevant passages	Relevant to claim No.
A	US 5270923 A (KEVIN F. KING T AL), 14 December 1993 (14.12.93), abstract -- --------	1-9

INTERNATIONAL SEARCH REPORT

Information on patent family members

29/04/98

International application No.
PCT/SE 98/00029

Patent document cited in search report	Publication date	Patent family member(s)	Publication date
US 5544212 A	06/08/96	EP 0713678 A	29/05/96
		JP 8215188 A	27/08/96
		EP 0648468 A	19/04/95
		JP 7178079 A	18/07/95
		US 5396418 A	07/03/95
		US 5485493 A	16/01/96
		EP 0587334 A	16/03/94
		JP 6205771 A	26/07/94
		DE 69128114 D,T	05/03/98
		EP 0471455 A,B	19/02/92
		EP 0713677 A	29/05/96
		JP 6125890 A	10/05/94
		US 5262946 A	16/11/93
		DE 68917846 D,T	22/12/94
		EP 0365301 A,B	25/04/90
		JP 2249535 A	05/10/90
		US 4947412 A	07/08/90
		US 4965726 A	23/10/90
		US 5166961 A	24/11/92
		US 5228070 A	13/07/93
		EP 0429191 A	29/05/91
		JP 3172975 A	26/07/91
		US 5276614 A	04/01/94
US 5390112 A	14/02/95	NONE	
US 5270923 A	14/12/93	CA 2021624 A	03/05/91
		EP 0426464 A	08/05/91
		IL 96050 A	05/12/96
		JP 1931924 C	12/05/95
		JP 3168124 A	19/07/91
		JP 6061326 B	17/08/94